

# High Temperature Behavior of Cr<sub>3</sub>C<sub>2</sub>-NiCr Coatings in the Actual Coal-Fired Boiler Environment

RAKESH BHATIA, HAZOOR SINGH SIDHU, and BUTA SINGH SIDHU

Erosion-corrosion is a serious problem observed in steam-powered electricity generation plants, and industrial waste incinerators. In the present study, four compositions of Cr<sub>3</sub>C<sub>2</sub>-(Ni-20Cr) alloy coating powder were deposited by high-velocity oxy-fuel spray technique on T-91 boiler tube steel. The cyclic studies were performed in a coal-fired boiler at 1123 K ± 10 K (850 °C ± 10 °C). X-ray diffraction, scanning electron microscopy/energy dispersive X-ray analysis and elemental mapping analysis techniques were used to analyze the corrosion products. All the coatings deposited on T-91 boiler tube steel imparted hot corrosion resistance. The 65 pctCr<sub>3</sub>C<sub>2</sub> -35 pct (Ni-20Cr)-coated T-91 steel sample performed better than all other coated samples in the given environment.

DOI: 10.1007/s40553-015-0045-x

© ASM International (ASM) and The Minerals, Metals & Materials Society (TMS) 2015

## I. INTRODUCTION

AN increasing demand for electricity, guidelines for reduced plant emissions, and a need of greater efficiency is forcing power plants to increase the steam pressure and temperature. Efforts are being made to further improve the efficiency of the boilers.<sup>[1,2]</sup> Materials used for high temperature applications are subjected to various types of degradation phenomenon such as high temperature corrosion, erosion-corrosion, overheating, solid particle abrasion, wear, etc. High-temperature corrosion of boiler tubes used for superheaters and reheaters in steam-generating systems has been recognized as a severe problem, resulting in tube wall thinning and premature failure. Attempts to decrease the maintenance costs of these components have increased interest in shielding them with protective coatings.<sup>[3,4]</sup>

Coal is an attractive fuel owing to its low price linked to its worldwide availability and due to the future shortage of other fossil fuel reserves such as oil and gas. But combustion of coal generates very corrosive media particularly near the superheater tubes.<sup>[3,5]</sup> Most corrosion problems stem from the coal feed. Coal can vary in its detailed composition of the impurities which contribute to its corrosivity.<sup>[6]</sup> Unaccepted levels of surface degradation of metal containment walls and heat exchanger tubing by a combined erosion-corrosion (E-C) mechanism have been experienced in some boilers, particularly fluidized bed combustors.<sup>[7]</sup> According to a study conducted by Levy, a dynamic surface layer is

formed that consists of a mechanical mixture of particles from the boiler gases and oxide scale growing from the base metal. It is constantly being refurbished and removed at a rate that results in an essentially constant thickness of the deposit/scale layer during steady state operation of the boiler; thereby, loss of sound metal is related to the rate of oxidation of the metal.<sup>[7]</sup>

Erosion-corrosion is the combined action of flow and corrosion, leading to an accelerated rate of loss of material. High temperature corrosion is the attack of metal surfaces that results from the combined effect of dry oxidation, sulphidation and/or high temperature chloride attack, or the dissolution of a metal or alloy by lower melting-point salts such as potassium, sodium and vanadium salts, at temperatures above about 623 K (350 °C).<sup>[4]</sup>

Composite materials are able to meet such a demanding spectrum of requirements, the base material provides the necessary mechanical strength and coatings provide a way of extending the limits of use of materials at higher temperatures.<sup>[8,9]</sup> Coatings provide a way of extending the limits of use of materials at the upper end of their performance capabilities, by allowing the mechanical properties of the substrate material to be maintained while protecting them against wear or corrosion.<sup>[8]</sup> High-velocity oxy-fuel (HVOF) processes belong to the family of thermal spraying technologies and are capable of producing coatings with high hardness, low oxidation, high abrasion resistance, low porosity and high erosion resistance compared to the other thermal spray-coating processes.<sup>[10-14]</sup> HVOF-spraying is a relatively new, economical and rapidly growing thermal spray technique for depositing cermets, metallic and ceramic protective overlay coatings onto engineering components to allow them to function under extreme conditions.<sup>[15,16]</sup> Cr<sub>3</sub>C<sub>2</sub>-NiCr cermet coatings have been extensively used to mitigate abrasive and erosive wear at high temperatures up to 1123 K (850 °C).<sup>[17,18]</sup> The corrosion resistance is provided by

RAKESH BHATIA, Assistant Professor, and HAZOOR SINGH SIDHU, Associate Professor, are with the Yadavindra College of Engineering, Punjabi University, G.K.Campus, Talwandi Sabo, Bathinda, Punjab 151302, India. Contact e-mail: hazoors@yahoo.com BUTA SINGH SIDHU, Dean Academics, is with the Punjab Technical University, Jalandhar-Kapurthala Highway, Kapurtala Punjab, India.

Manuscript submitted May 30, 2014.

Article published online February 18, 2015

**Table I. Chemical Composition (Weight Percent) of Boiler Tube Steel (T-91)**

Nb	Mn	Si	Cr	Mo	Ni	C	Fe
0.07	0.5	0.4	9	0.95	0.4	0.11	Balance

the NiCr matrix while the wear resistance is mainly due to the carbide ceramic phase.<sup>[19]</sup>

Although satisfactory results have been obtained with cermet coating systems, a great deal of debate still persists over the best hard phase matrix ratio for optimum erosion resistance. The erosion resistance of cermet coatings increases with an increase in chromium carbide in the pre-sprayed powder. Researchers agree that carbide-based coatings provide excellent erosion protection, but disagree on the optimum amount of carbide for maximum erosion resistance.<sup>[20-22]</sup>

The present investigation aimed to evaluate the degradation behaviour of HVOF-sprayed Cr<sub>3</sub>C<sub>2</sub>-NiCr coatings on boiler tube steel in an actual industrial environment. The X-ray diffractometer, SEM/EDAX and EPMA analysis techniques have been used for analysis purposes. The erosion-corrosion rates have been monitored in terms of thickness lost.

## II. EXPERIMENTAL

### A. Substrate Material

The boiler tube steel T-91 with chemical composition as shown in Table I have been used as substrate material. The tube material was obtained from Guru Nanak Dev Thermal Power Plant, Bathinda, and samples with dimensions 22 mm × 15 mm × 3 mm were prepared.

### B. Formulation of Coating

Commercially available compositions of 65 pctCr<sub>3</sub>C<sub>2</sub>-35 pct (Ni-20Cr), 75 pct Cr<sub>3</sub>C<sub>2</sub>-25 pct (Ni-20Cr), 80 pct Cr<sub>3</sub>C<sub>2</sub>-20 pct (Ni-20Cr) and 90 pct Cr<sub>3</sub>C<sub>2</sub>-10 pct (Ni-20Cr) alloy powders were used for formulating the coatings. The designations of the coatings are given in Table II. The coatings were developed at M/S Metallizing Equipment (Jodhpur, India) by using a commercial Hipojet-2100 HVOF thermal spray system. Details of coating parameters have been published elsewhere.<sup>[22]</sup> The average thickness, porosity and microhardness of the developed coatings are evaluated and reported in Table III.

### C. Erosion-Corrosion (E-C) Studies in an Actual Boiler Environment

The E-C studies in an actual boiler environment were conducted at Guru Nanak Dev thermal power plant, Bathinda, Punjab, India. A hole of 2 mm diameter was drilled in the uncoated and coated samples to hang in the boiler for erosion-corrosion studies. Nichrome wire was used to hang the samples in the boiler at 1123 K ± 283 K (850 °C ± 10 °C) with a full load of

**Table II. Designation of Coating Powders Used in the Study**

Coating Powder	Coating Designation
65 pctCr <sub>3</sub> C <sub>2</sub> -35 pct (Ni-20Cr)	CC1
75 pctCr <sub>3</sub> C <sub>2</sub> -25 pct (Ni-20Cr)	CC2
80 pctCr <sub>3</sub> C <sub>2</sub> -20 pct(Ni-20Cr)	CC3
90 pctCr <sub>3</sub> C <sub>2</sub> -10 pct (Ni-20Cr)	CC4

**Table III. Thickness, Porosity and Average Microhardness of Different Coated Samples**

Coating	Average Thickness	Porosity (Pct)	Average Microhardness (H <sub>v</sub> )
Uncoated T-91	—	—	317
CC4	375 μm	<2 pct	1167
CC3	325 μm	<1.8 pct	887
CC2	350 μm	<1.5 pct	862
CC1	350 μm	< 1.5 pct	688

110 MW. The samples were inserted in the boiler unit-II through the soot blower dummy point at 31 m height from the base of the boiler. The studies were conducted for 15 cycles; each cycle consisted of 100 hours exposure to the boiler environment followed by 1 hour cooling at ambient conditions. Visual observations were made after the end of each cycle with respect to colour, luster or any other physical aspect of the oxide scale formed. The mass change data were taken after each cycle along with physical observations to approximate the kinetics of E-C. However, in this environment, the mass change data alone could not be of much use for predicting E-C behavior because of suspected spalling and ash deposition on the samples. Therefore, the extent of E-C has also been evaluated by measuring the thickness of the scale lost due to erosion, spalling or evaporation by finding the difference in thickness of the specimens before and after 1500 hours exposure to the actual environment. The thickness was measured using digital micrometer ( resolution 0.01 mm; Mitutoyo, Japan) and each reported value is the average of 5 measured values at three different locations.

## III. RESULTS

### A. Visual Examination

The macrograph of uncoated T-91 boiler tube steel and the coated samples after 1500 hours exposure in the coal-fired boiler is shown in Figure 1. Uncoated T-91 boiler tube steel changed to blackish grey after the very 1st cycle of exposure. This might be due to the formation of oxides. A layer of ash was seen to be

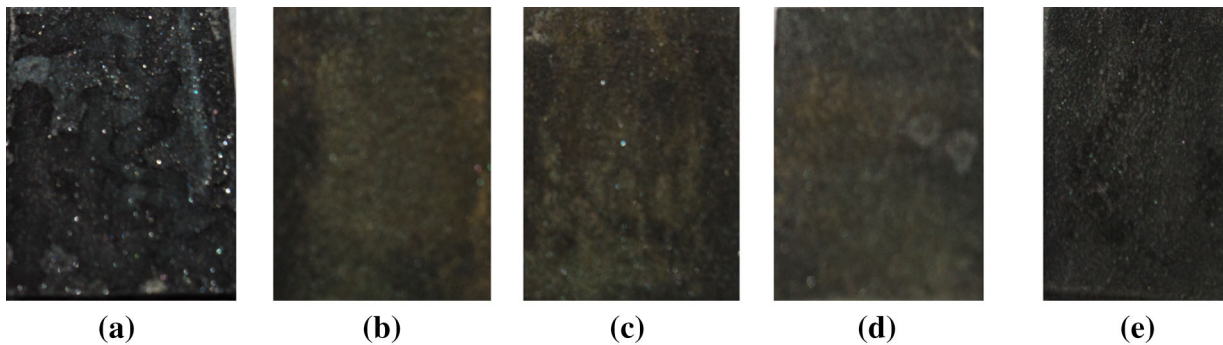


Fig. 1—Macrograph of the samples subjected to an actual boiler environment at 1123 K (850 °C) for 1500 h: (a) uncoated, (b) CC1, (c) CC2, (d) CC3, and (e) CC4.

deposited on the surface and the surface seems to be rough. The colour of the sample turned dark black by the end of the 2nd cycle. This might be due to the formation of oxides. The process of scale formation seems to increase by the end of the 5th cycle and a shining black colour was observed at the corners of the sample at the end of the 6th cycle. The process of scale formation and spalling of scale continued until the 15th cycle. The colour of the CC1-coated T-91 boiler tube steel sample turned blackish grey at the end of the 1st cycle. This might be due to formation of oxides of Cr and Ni. The coating was found to be intact with ash deposits without any cracks appearing in the surface of the sample. The surface of the coating appeared to be smooth at the end of the 2nd cycle. No signs of spallation were observed throughout the study, the CC2-coated sample turned light blackish grey with ash deposits on all the surfaces. The colour turned dark black by the end of the 5th cycle and with the progress of the experiment the colour further darkened to dark grey. No visible cracks were observed on the surfaces of specimens during or after the exposure of 1500 hours. A thin layer of scale can be observed at the top surface. The scale formed on the coated sample was found to be intact without any spallation. A light blackish grey colour at the end of the 1st cycle was observed for CC3 sample. Ash deposits were also seen at the surface of the sample. At the end of the study, the coating was found to be intact with a visible layer of scale and without any visual cracks. The colour of the CC4-coated sample turned light blackish grey by the end of the 1st cycle, and to dark black by the end of the 3rd cycle, indicating the formation of oxides. The formation of scale started and progressed slowly with no major or minor cracks appearing on the surface until the 15th cycle.

### B. Thickness Loss Monitoring

The weight change data in this case cannot be used for predicting the erosion-corrosion behaviour because of spalling of the scale and ash deposition on the samples during testing. So, the extent of erosion-corrosion in this case was monitored by measuring the thickness of the unreacted sample after the total exposure of 1500 hours. The thickness lost due to the exposure in the boiler for 1500 hours and the corrosion rate calculated based

**Table IV. Thickness Loss and Corrosion Rate of the Coatings Subjected to an Actual Boiler Environment at 1123 K (850 °C) for 1500 h**

Sample	Thickness Loss (mm)	Corrosion Rate [Mils Per Year (mpy)]
uncoated	0.36	82.8
CC1	0.014	3.22
CC2	0.022	5.06
CC3	0.029	6.67
CC4	0.034	7.82

upon thickness-loss data [in term of mils per year (mpy)] for uncoated and coated T-91 boiler tube steel samples are reported in Table IV.

### C. X-ray Diffraction Analysis

The XRD analysis of the oxide scale of uncoated and coated T-91 boiler tube steel samples exposed to the erosion-corrosion at 1123 K (850 °C) for 15 cycles is shown in Figures 3(a)–(e). Oxide scale of the uncoated steel mainly comprise  $\text{Fe}_2\text{O}_3$  phase along with weak intensity of  $\text{Al}_2\text{O}_3$  and  $\text{Na}_2\text{C}_6\text{O}_6$  phase. Some weak peaks corresponding to  $\text{Cr}_2\text{O}_3$  have also been observed.

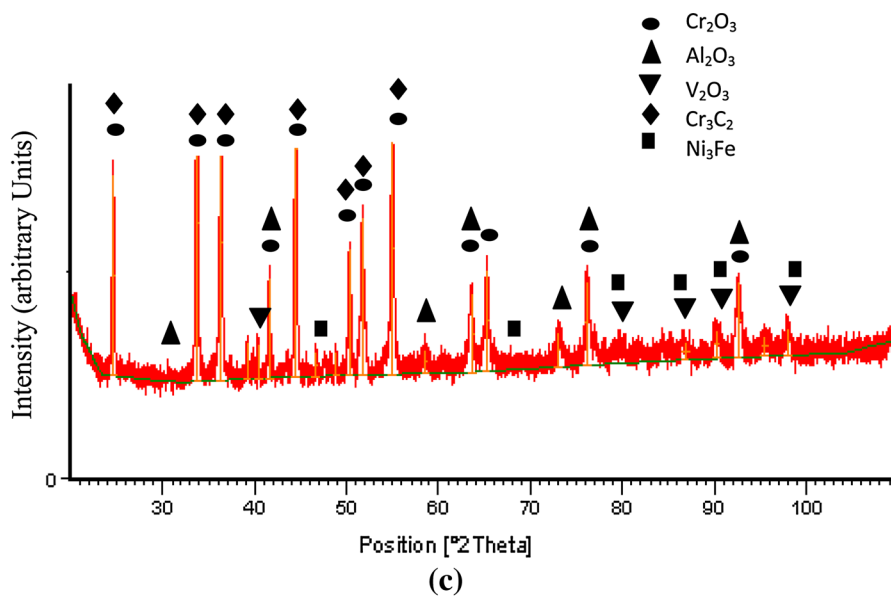
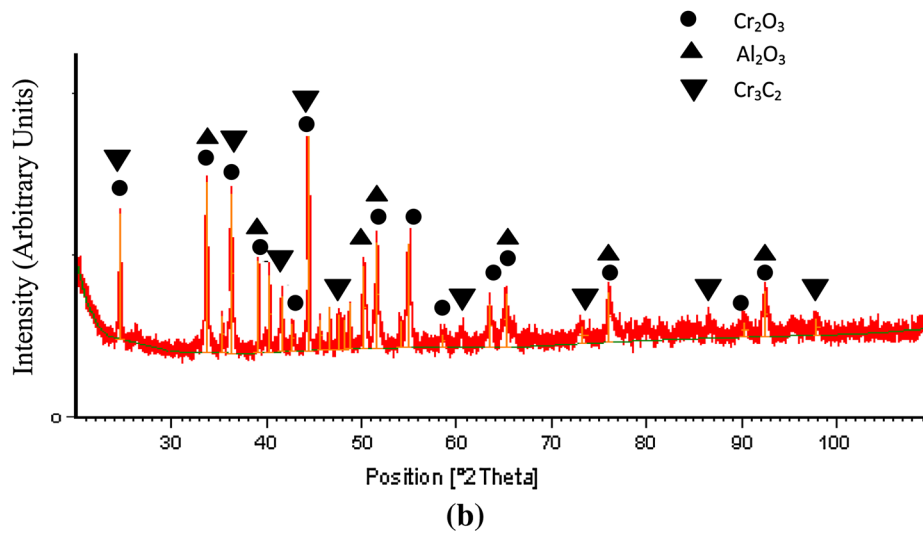
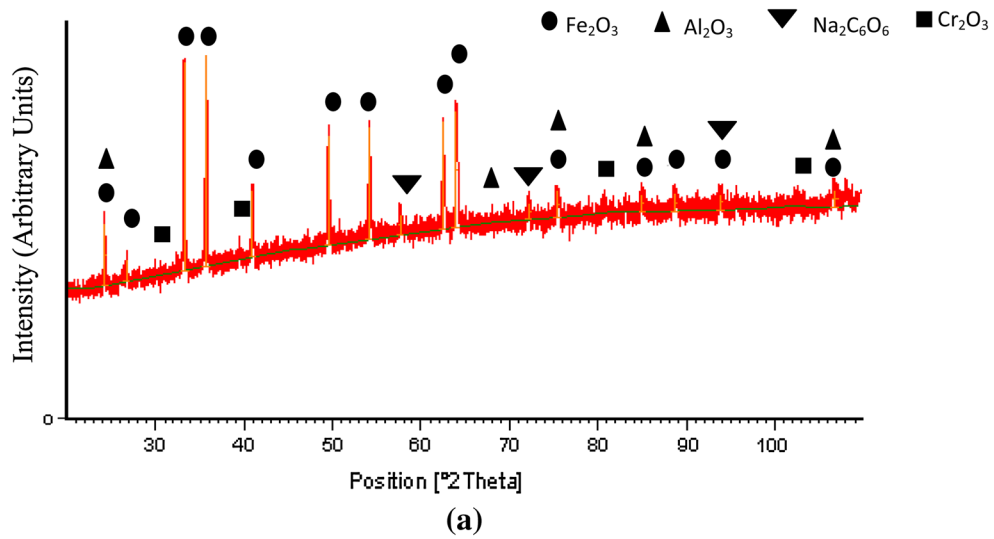
The XRD analysis of the oxide scale of the coated sample exposed to the erosion-corrosion mainly comprise phases of  $\text{Cr}_2\text{O}_3$  and  $\text{Al}_2\text{O}_3$ , along with some weak peaks of  $\text{Cr}_3\text{C}_2$ ,  $\text{Ni}_3\text{Fe}$ ,  $\text{V}_2\text{O}_5$ ,  $\text{Fe}_2\text{O}_3$ ,  $\text{Cr}_7\text{C}_3$  and  $\text{SiO}_2$  phases.

### D. FE-SEM/EDS Analysis

#### 1. Surface morphology

The oxide scale for the uncoated T-91 shown in Figure 3(a) seems to have a granular morphology. The EDS analysis reveals that the scale mainly contains Fe and O, with significant amounts of C. Significant amounts of Si and Al are also observed. Minor amounts of Na and K are also visible throughout the scale, which are the basic constituents of the boiler environment.

FE-SEM analysis of the CC1-coated T-91 boiler tube steel sample subjected to the boiler environment shows uneven scale morphology as shown in Figure 3(b). Granular growth of oxide scale is evident from the





◀ Fig. 2—(a) X-ray diffraction profiles for the uncoated boiler tube steel subjected to an actual boiler environment at 1123 K (850 °C) for 1500 h. (b) X-ray diffraction profiles for the CC1-coated T-91 boiler tube steel subjected to an actual boiler environment at 1123 K (850 °C) for 1500 h. (c) X-ray diffraction profiles for the CC2-coated T-91 boiler tube steel subjected to an actual boiler environment at 1123 K (850 °C) for 1500 h. (d) X-ray diffraction profiles for the CC3-coated T-91 boiler tube steel subjected to an actual boiler environment at 1123 K (850 °C) for 1500 h. (e) X-ray diffraction profiles for the CC4-coated T-91 boiler tube steel subjected to an actual boiler environment at 1123 K (850 °C) for 1500 h.

Significant amounts of Si and Al were also noticed at the points of investigation. A marginal presence of V can also be noticed on the surface of the sample. Protective oxides of Cr and Ni might have been formed at the surface after the exposure.

Figure 3(c) shows the growth of oxide scale on the surface of the CC2-coated T-91 boiler tube steel sample after exposure to the boiler environment. Some tiny spherical particles are also seen at many places on the surface of the sample. The EDS analysis reveals the presence of a high percentage of Cr at all the points of investigation. FE-SEM analysis of the CC3-coated T-91 boiler tube steel sample is presented in Figure 3(d). The EDS analysis reveals the presence of O, C, Cr, Fe and Ni as the main elements, with minor amounts of Si, Al, and V.

FE-SEM analysis of the CC4-coated T-91 boiler tube steel sample subjected to the boiler environment shows uneven scale morphology as shown in Figure 3(e). Growth of oxide scale along with signs of spalling of

FE-SEM analysis on the surface after exposure to boiler environment. Some tiny spherical particles along with irregular shaped particles are also seen on the surface of the sample at many places. The EDS analysis reveals the presence of high percentage Cr at all the points of investigation. Fe percentage is below 2 pct at all points. C and O are present in significant percentages with maximum percentage as 19 and 24 pct, respectively.

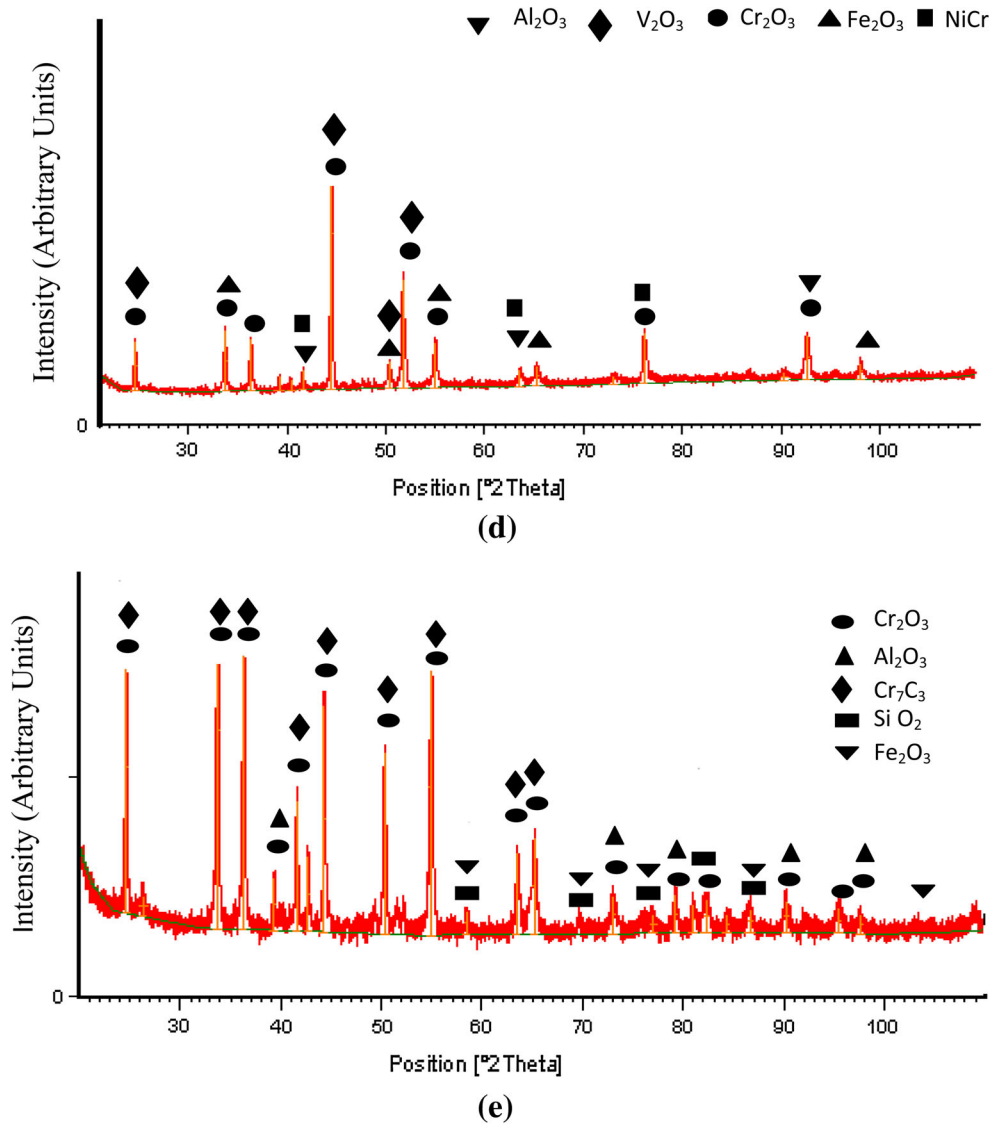
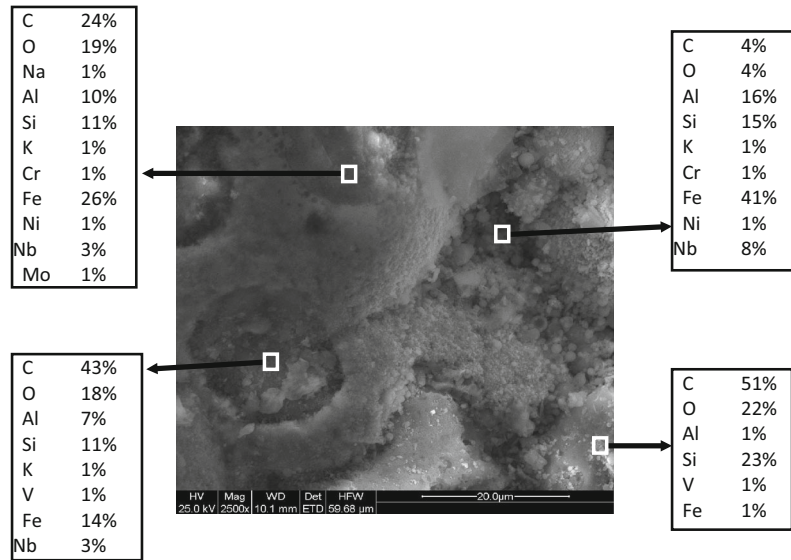
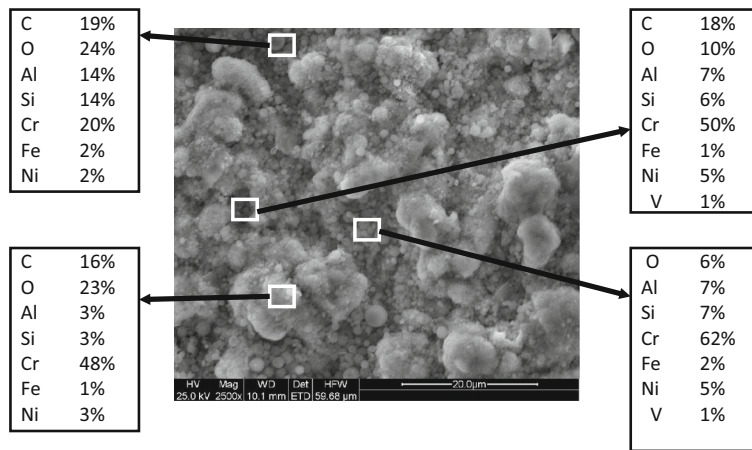


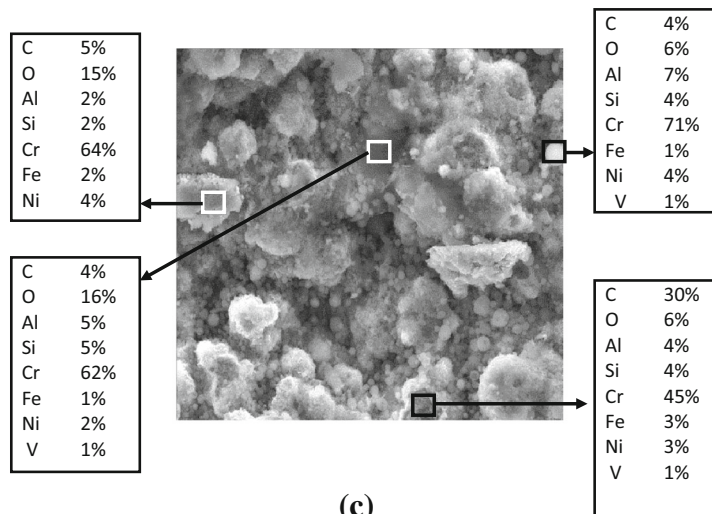
Fig. 2—continued.



(a)



(b)



(c)

◀Fig. 3—(a) FE-SEM along with EDS analysis for the uncoated T-91 boiler tube steel subjected to an actual boiler environment at 1123 K (850 °C) for 1500 h. (b) FE-SEM along with EDS analysis for the CC1-coated T-91 boiler tube steel sample subjected to an actual boiler environment at 1123 K (850 °C) for 1500 h. (c) FE-SEM along with EDS analysis for the CC2-coated T-91 boiler tube steel sample subjected to an actual boiler environment at 1123 K (850 °C) for 1500 h. (d) FE-SEM along with EDS analysis for the CC3-coated T-91 boiler tube steel sample subjected to an actual boiler environment at 1123 K (850 °C) for 1500 h. (e) FE-SEM along with EDS analysis for the CC4-coated T-91 boiler tube steel sample subjected to an actual boiler environment at 1123 K (850 °C) for 1500 h.

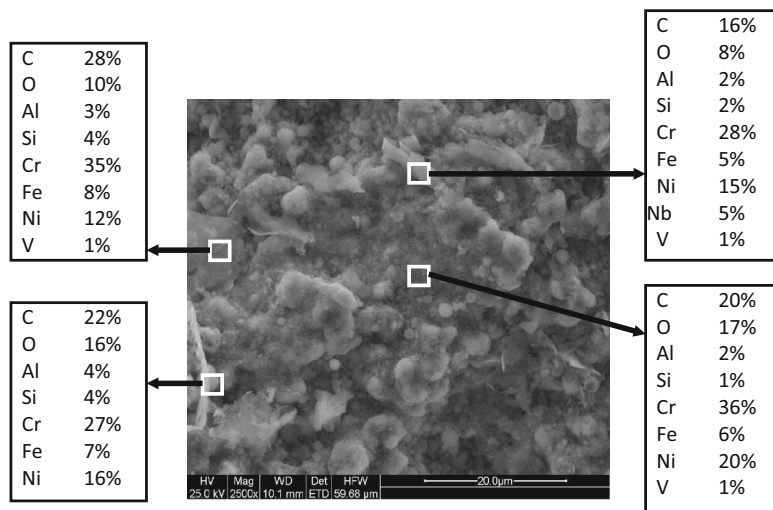
scale can be clearly seen in the micrograph. A high percentage of Cr is reported at almost all the points of the investigation. The presence of Ni analysed by EDS comes out as a maximum 5 pct and minimum 1 pct. High percentages of C and O are also reported in EDS analysis. Marginal amounts of Si, Al and V can also be seen in the analysis. A high percentage of Cr at the surface validates the formation of  $\text{Cr}_2\text{O}_3$ . Apart

from oxides of Cr, the formation of oxides of Ni, Si, Al might have taken place at the surface.

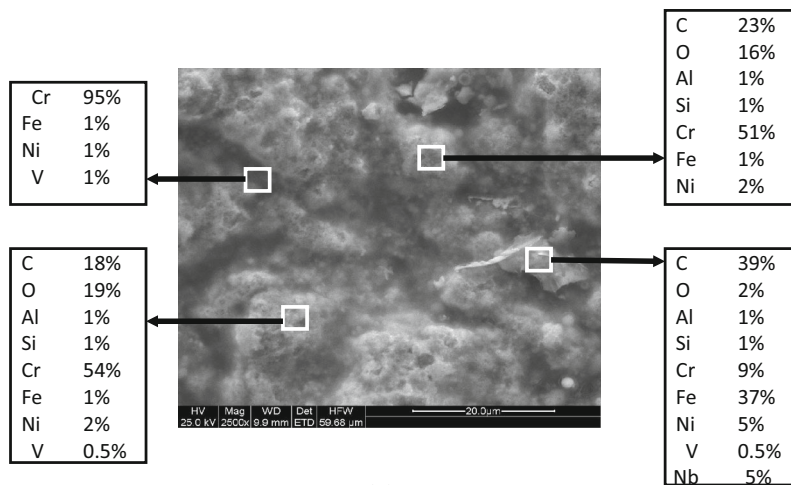
### E. Cross-Sectional Analysis

The FE-SEM micrograph in Figure 4(a) shows the uncoated sample with a thick oxide scale having cracks appearing in both parallel and perpendicular directions with respect to the substrate. Spallation of scale can also be observed with the scale breaking in shapes of granular particles due to the exposure. The cross-sectional oxide scale is mainly rich in Fe and O. Fe content is very high in the intact part of the substrate. Significant amounts of Cr and C are also visible at all points of the investigation along with Nb and Mo. Minor amounts of Na, K and V (up to 1 pct) have also been observed.

The scale morphology and EDS analysis for the corroded cross-section of CC1-coated steel sample (Figure 4(b)) shows a high weight percentage of Fe in

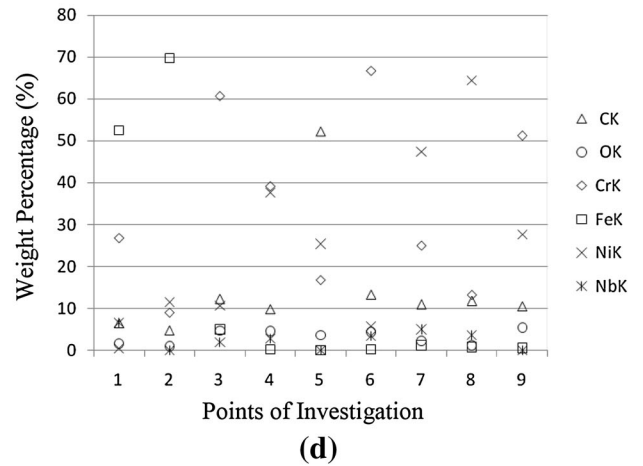
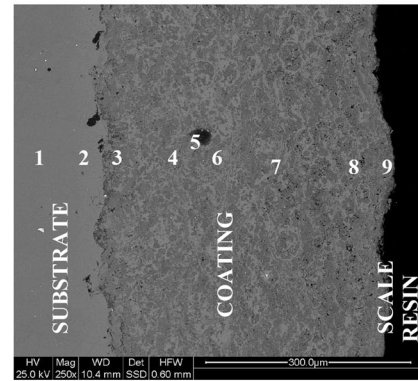
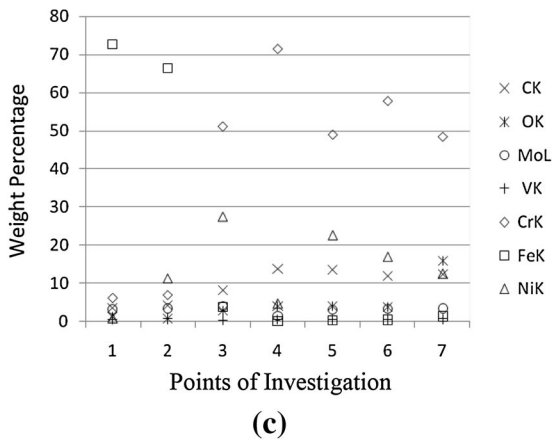
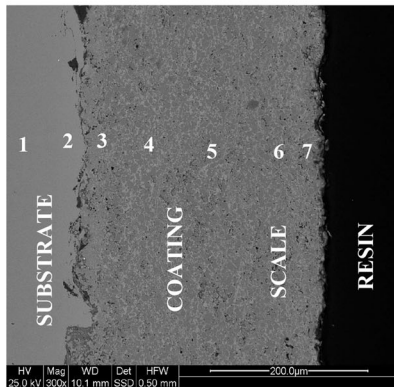
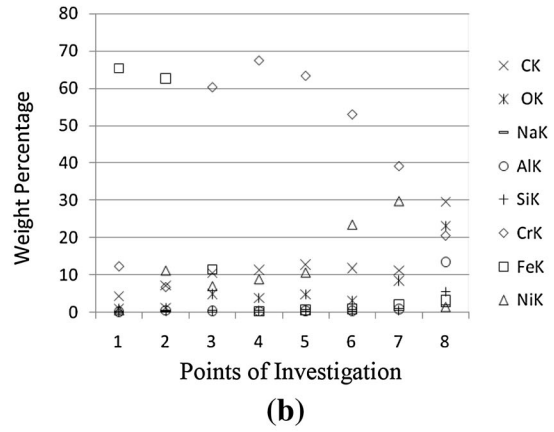
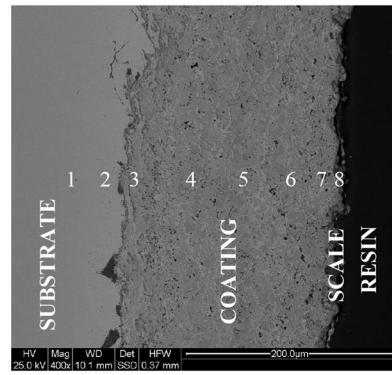
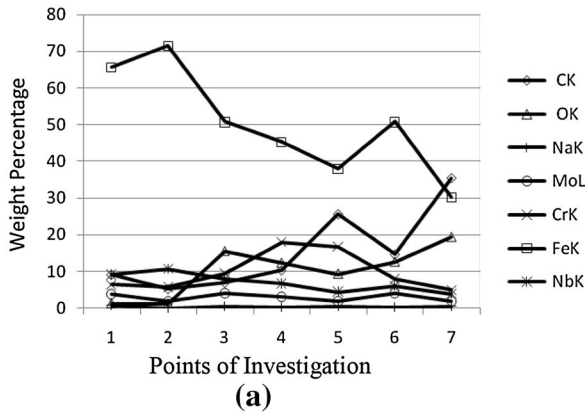
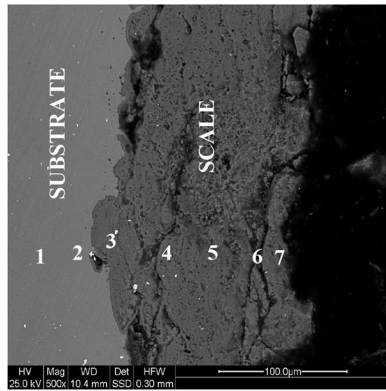


(d)



(e)

Fig. 3—continued.





◀ Fig. 4—(a) Oxide scale morphology and variation of elemental composition across the cross-section of uncoated T-91 boiler tube steel subjected to an actual boiler environment at 1123 K (850 °C) for 1500 h. (b) Oxide scale morphology and variation of elemental composition across the cross-section of the CC1-coated T-91 boiler tube steel sample subjected to an actual boiler environment at 1123 K (850 °C) for 1500 h. (c) Oxide scale morphology and variation of elemental composition across the cross-section of the CC2-coated T-91 boiler tube steel sample subjected to an actual boiler environment at 1123 K (850 °C) for 1500 h. (d) Oxide scale morphology and variation of elemental composition across the cross-section of the CC3-coated T-91 boiler tube steel sample subjected to an actual boiler environment at 1123 K (850 °C) for 1500 h. (e) Oxide scale morphology and variation of elemental composition across the cross-section of the CC4-coated T-91 boiler tube steel sample subjected to an actual boiler environment at 1123 K (850 °C) for 1500 h.

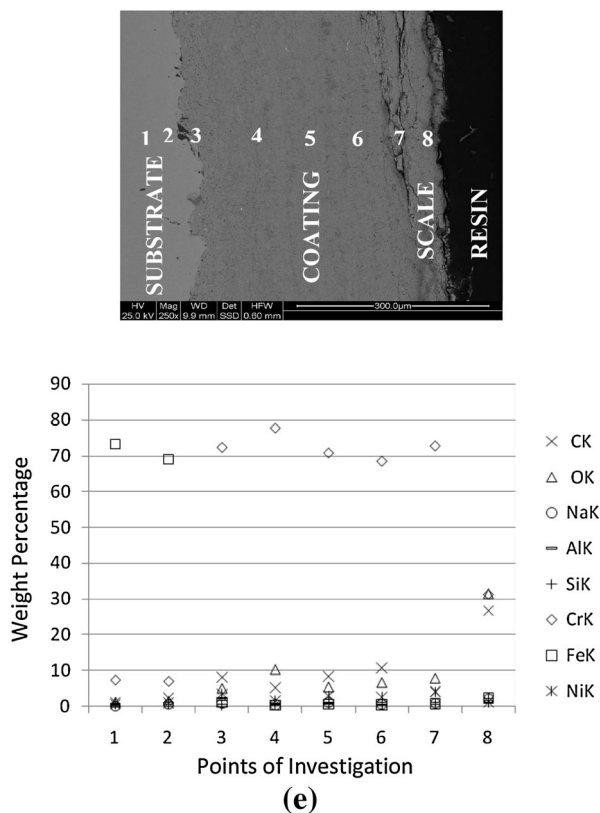


Fig. 4—continued.

substrate (65 and 62 pct at points 1 and 2, respectively) and a rich content of Cr and Ni in the coating area with maximum percentages of 67 and 29 pct, respectively. The EDS analysis show the topmost layer consisting of Cr (20 pct) and Al (13 pct) along with C (29 pct) and O (23 pct). The analysis indicates the formation of protective oxides of Cr and Ni, along with  $Al_2O_3$ .

A thin layer of oxide scale at the top surface of the CC2 coating can be seen in the micrograph (Figure 4(c)). Significant amounts of Cr and Ni are present in the coating areas from point 3 onwards, whereas the content percentage of Fe is marginal in the coating. Maximum amounts of O (15 pct) can be seen in the EDS analysis at the top layer at point 7 whereas at all other points the weight percentage is marginal. The

presence of Mo in low percentage amounts can also be seen along the cross-section at all the points.

The FE-SEM micrograph (Figure 4(d)) indicates almost negligible thickness of oxide scale at the top surface of CC3 coating. Low amounts of O can also be seen at all points of investigation, with maximum amounts (5 pct) available at the top layer (point 9). Very high percentages of Cr (51 pct) and Ni (27 pct) can also be visualised in the analysis indicating the formation of protective spinels of Cr and Ni.

The scale morphology and EDS analysis for the corroded cross-section of CC4-coated T-91 boiler tube steel sample after exposure to the boiler environment is shown in Figure 4(e). A dense and uniform scale is visible in the micrograph. The Cr content in the coating is almost 70 pct at all the points except at point 8, the top layer of oxide scale. At the top surface, the weight percentage of the elements is C (26 pct), O (31 pct), Cr (31 pct), Ni (1 pct), Fe (2 pct), Na (2 pct) and Al and Si (1 pct). The weight percentage of O is highest at point 8, the top layer of the scale. EDS analysis across the cross-section of the sample validates the formation of  $Cr_2O_3$ , NiO and  $Fe_2O_3$  at the top oxide layer, along with oxides of Si and Al. The coating has developed cracks parallel to the substrate surface.

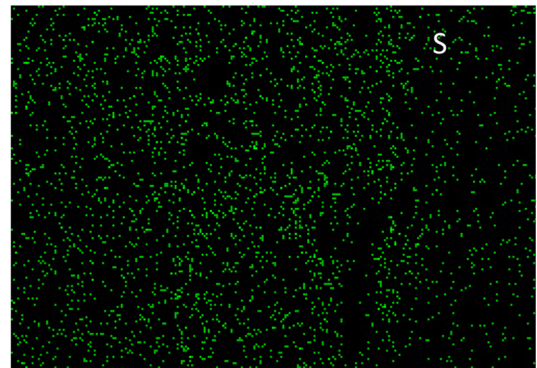
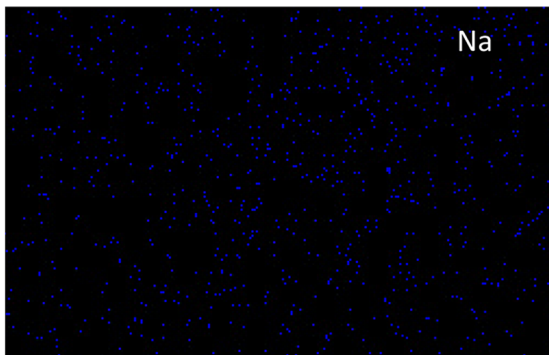
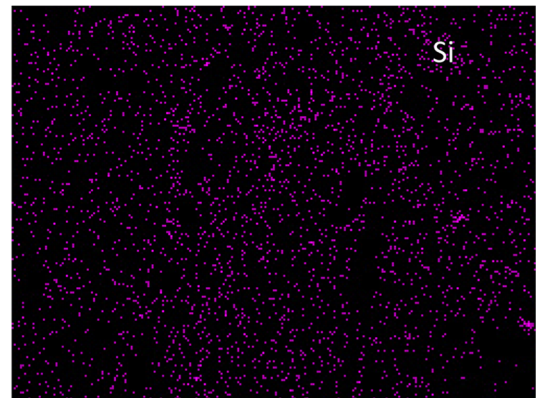
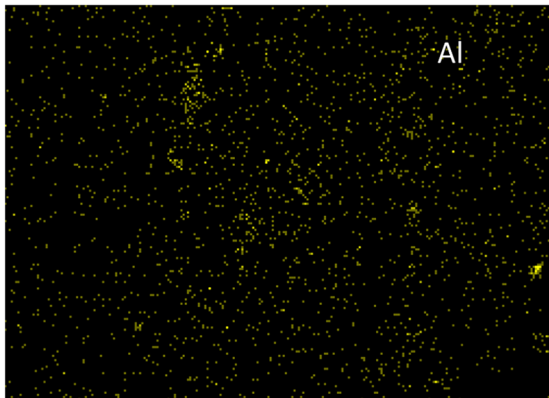
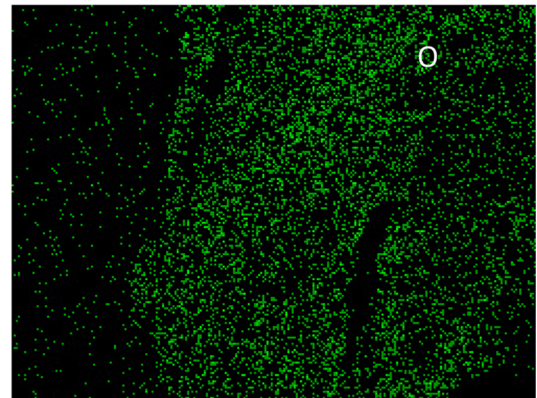
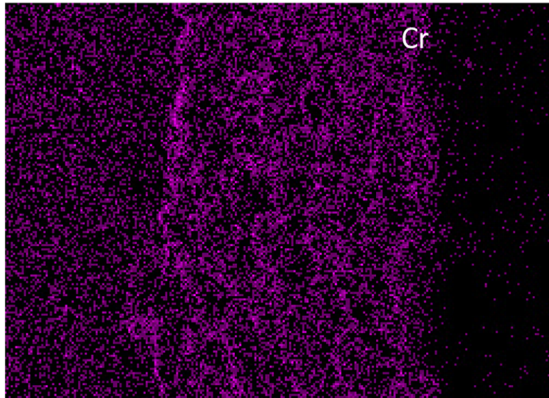
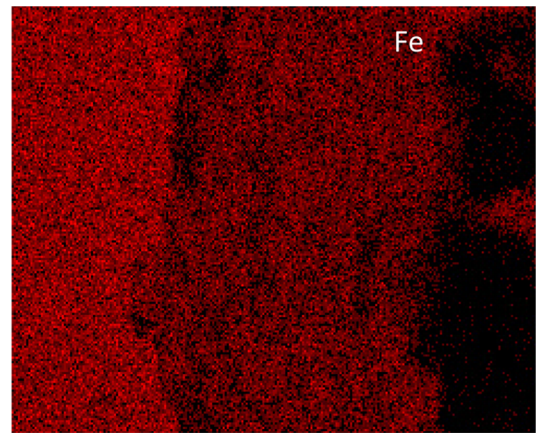
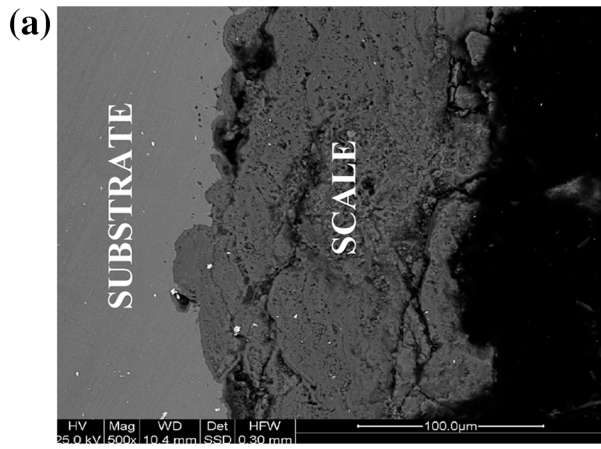
#### F. Elemental Mapping Analysis

Composition image (SEI) and X-ray mappings of the cross-section of uncoated and coated T-91 boiler tube steel samples subjected to actual boiler environments at 1123 K (850 °C) for 1500 hours are depicted in Figures 5(a)–(e). The oxide scale of uncoated T-91 shown in Figure 5(a) is in general rich in Fe, Cr and O. Cr along with O can be seen penetrating towards the substrate. Na and Al particles are visible on the surface. The overall oxide scale mainly consists of Fe, Cr and O, indicating the formation of  $Fe_2O_3$  and  $Cr_2O_3$  in the scale.

X-ray mappings for a part of the oxide scale of the HVOF-sprayed CC1-coated T-91 boiler tube steel sample are shown in Figure 5(b). The analysis indicates the top surface mainly contains Cr and Ni. Some localized areas which are rich in Cr are depleted of Ni. Spots of Al can be seen at the coating–substrate interface; at these points, the substrate material seems to be eroded by striking of Al particles. The oxide scale for the coating is found to have a Ni- and Cr-rich layer.

X-ray mappings analysis of the oxide scale of the CC2-coated steel sample indicates a very thin layer of oxide scale at the top surface. A very thin layer of Fe can be seen to be present in the mapping at the topmost outer layer of the scale along with O, indicating the presence of a  $Fe_2O_3$  non-protective oxide. The coating was found to be rich in Ni and Cr. A thin layer of Al can be seen at the top surface and at the coating–substrate interface. The attack of corrosive species like V and S can also be visualized in the mappings, as S and V can be seen penetrating towards the substrate.

Figure 5(d) indicates the uniform distribution of O in the coating area with a thick layer at the top surface. Rich content of Cr and Ni can also be seen in the





◀Fig. 5—(a) Composition image (SEI) and X-ray mappings of the cross-section of the uncoated T-91 boiler tube steel subjected to an actual boiler environment at 1123 K (850 °C) for 1500 h. (b) Composition image (SEI) and X-ray mappings of the cross-section of the CC1-coated T-91 boiler tube steel sample subjected to an actual boiler environment at 1123 K (850 °C) for 1500 h. (c) Composition image (SEI) and X-ray mappings of the cross-section of the CC2-coated T-91 boiler tube steel sample subjected to an actual boiler environment at 1123 K (850 °C) for 1500 h. (d) Composition image (SEI) and X-ray mappings of the cross-section of the CC3-coated T-91 boiler tube steel sample subjected to an actual boiler environment at 1123 K (850 °C) for 1500 h. (e) Composition image (SEI) and X-ray mappings of the cross-section of the 90 pctCr<sub>3</sub>C<sub>2</sub>-10 pct (Ni-20Cr)-coated T-91 boiler tube steel sample subjected to an actual boiler environment at 1123 K (850 °C) for 1500 h.

coating area to stop the attack of corrosive species. Vanadium can be seen to be present throughout the mapping indicating the attack due to burning of coal during combustion.

X-ray mappings for a part of the oxide scale of HVOF-sprayed CC4-coated T-91 boiler tube steel sample are shown in Figure 5(e). The BSE image shows cracks in the coating developed after exposure to the actual boiler environment. Apart from the substrate, a dense layer of Fe can also be seen at the top layer of the scale, indicating the formation of non-protective oxides of Fe<sub>2</sub>O<sub>3</sub>. The coating is found to be rich in Cr content as indicated in the mappings. Uniformly distributed Ni can also be visualized in the coating area. O can also be seen to be uniformly distributed in the coating with a thick dense layer at the top. Penetration of O along with S towards the substrate can be seen in the mappings to initiate the corrosion activities. Distribution of Al can also be seen in the mapping, as some dark spots of Al can be visualized at the coating–substrate interface and at the top layer of the scale. This might indicate the possibility of erosion of material by Al<sub>2</sub>O<sub>3</sub> particles.

## IV. DISCUSSION

### A. Uncoated T-91 Steel

The oxide scale for the uncoated T-91 seems to have a splintered morphology with tendency to spall. This indicates that the steel exhibited lower erosion-corrosion resistance. This is further evidence from the thickness loss data, according to which the corrosion rate for the uncoated T-91 steel is 82.8 mpy. Formation of Fe<sub>2</sub>O<sub>3</sub> is revealed by the X-ray diffractograms (Figure 2(a)). This is attributed to the reaction of iron with oxygen, since iron is the main constituent of the boiler steel. The FE-SEM analysis (Figure 3(a)) from the surface also validates the presence of Fe and O on the surface of the sample, which is further confirmed by EDS analysis from the cross-section in Figure 4(a), which shows Fe in very high percentage at points 3, 4, 5, 6 and 7 of the oxide scale layer along with a sufficient amount of O, indicating the formation of iron oxide. Formation of such types of oxide has also been analyzed by Sidhu *et al.*,<sup>[3]</sup> Prakash *et al.*,<sup>[23]</sup> Srikanth *et al.*,<sup>[24]</sup> Singh,<sup>[25]</sup> Bala,<sup>[26]</sup> Kaushal *et al.*,<sup>[27]</sup> and Kaur *et al.*<sup>[28]</sup>. The

presence of Fe<sub>2</sub>O<sub>3</sub> is further confirmed by EPMA analysis (Figure 5).

The presence of Al<sub>2</sub>O<sub>3</sub> might be due to the deposition of ash particles on the exposed samples. The XRD and EDS analysis shows the presence of ash deposited on the sample, which is further interacting with the oxide scale. The embedment of the ash particles in the scale of boiler tube steel has also been confirmed by the EPMA analysis. The presence of Al and Na as shown by X-ray maps indicates the presence of ash particles. Levy *et al.* and Sidhu *et al.* have also observed the presence of mixture of bed material constituents in the outer scale deposits during erosion corrosion of boiler steel tubing in combustion boiler environment<sup>[7,24,29]</sup>. The possibility of formation of such phases has further been reported by Sidhu *et al.*,<sup>[3]</sup> Nelson *et al.*,<sup>[6]</sup> Singh,<sup>[25]</sup> Bala,<sup>[26]</sup> Kaur *et al.*,<sup>[28]</sup> and Kaushal *et al.*<sup>[27,29]</sup>.

### B. Coated T-91 Samples

Based upon the thickness loss data and diffusion of Fe towards the top of oxide layer as shown in X-ray mappings (Figures 5(b)–(e)), the erosion-corrosion resistance of the coatings is as per the order

$$\text{CC1} > \text{CC2} > \text{CC3} > \text{CC4}.$$

CC1 coating proved to be effective in imparting the necessary protection to the T-91 boiler tube steel as the thickness loss observed is 0.014 mm for 1500 hours of exposure in the actual boiler environment. Moreover, the coating has shown no spallation during the erosion corrosion study. The SEM micrograph in Figure 4(b) shows compact and adherent surface scale consisting of oxides of Ni and Cr. Further, no crack or void is visible on the surface. A lesser thickness loss rate in the case of CC1-coated T-91 boiler tube steel exposed to the actual boiler environment might be attributed to the compact and less porous structure of its oxide scale. Sidhu *et al.*<sup>[30]</sup> reported that the more compact and less porous the coating, the higher its erosion-corrosion resistance. The scale has retained the lamellar structure of the coating and there is no indication of any crack along the cross-section of the scale. Hence, it can be inferred that the coating shows a tendency to act as a diffusion barrier to the corroding species in the environment of a coal-fired boiler. It is well known that Cr<sub>3</sub>C<sub>2</sub> particles impart the high erosion resistance and NiCr provides the necessary oxidation resistance. Chromium has higher affinity for oxygen than nickel and forms a more stable oxide, hence the formation of Cr<sub>2</sub>O<sub>3</sub> inhibits oxidation of the substrate alloys by blocking the diffusion of reacting species.<sup>[25,31–36]</sup>

Moreover, Cr<sub>2</sub>O<sub>3</sub> being of a significantly harder phase can also provide erosion resistance along with corrosion resistance. EDAX analysis from the cross-section verifies the presence of these elements at the top surface of the scale and shows that the oxides of Cr and Ni have been responsible for blocking the degrading species through the coating. The EPMA analysis shown in

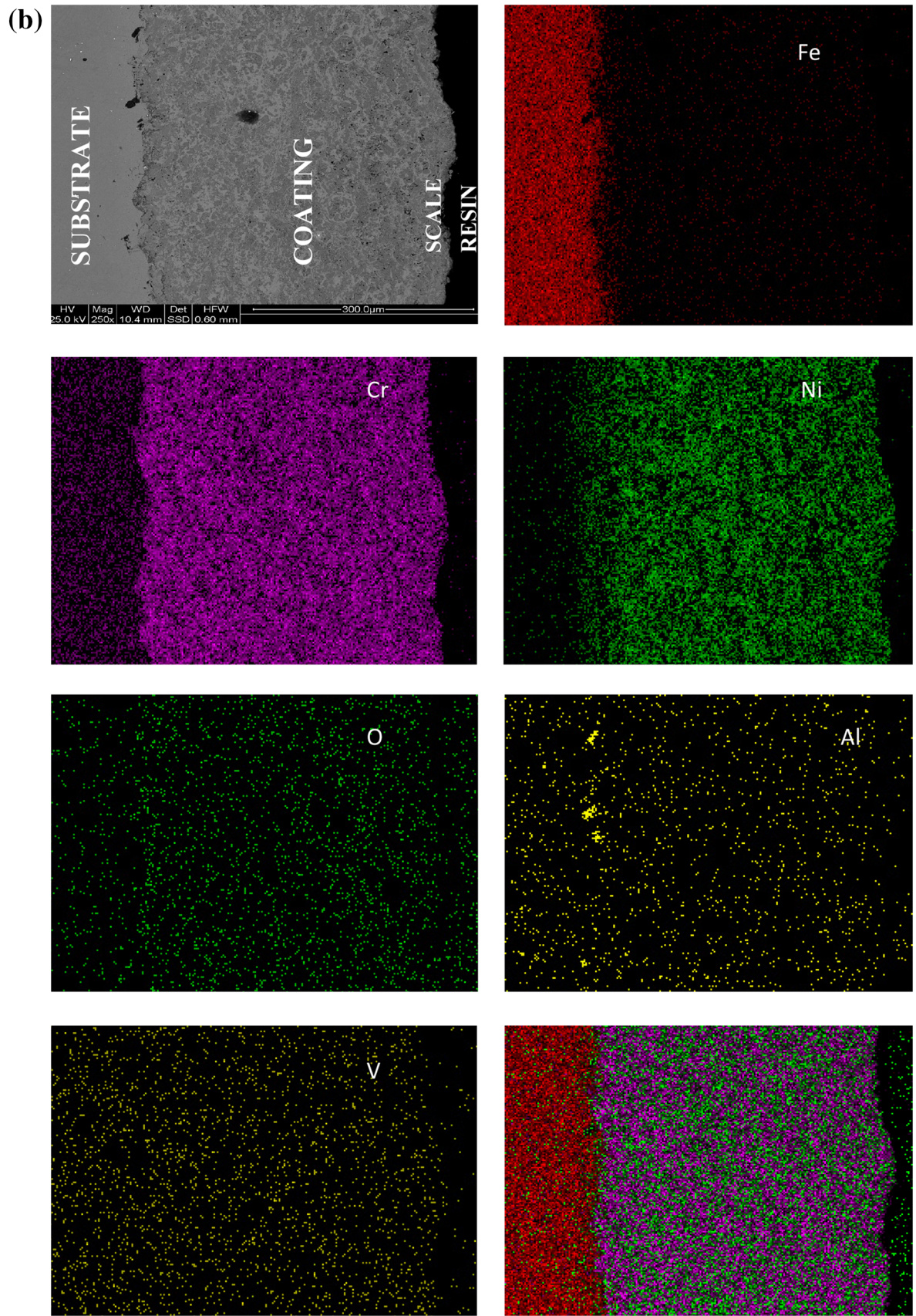


Fig. 5—continued.



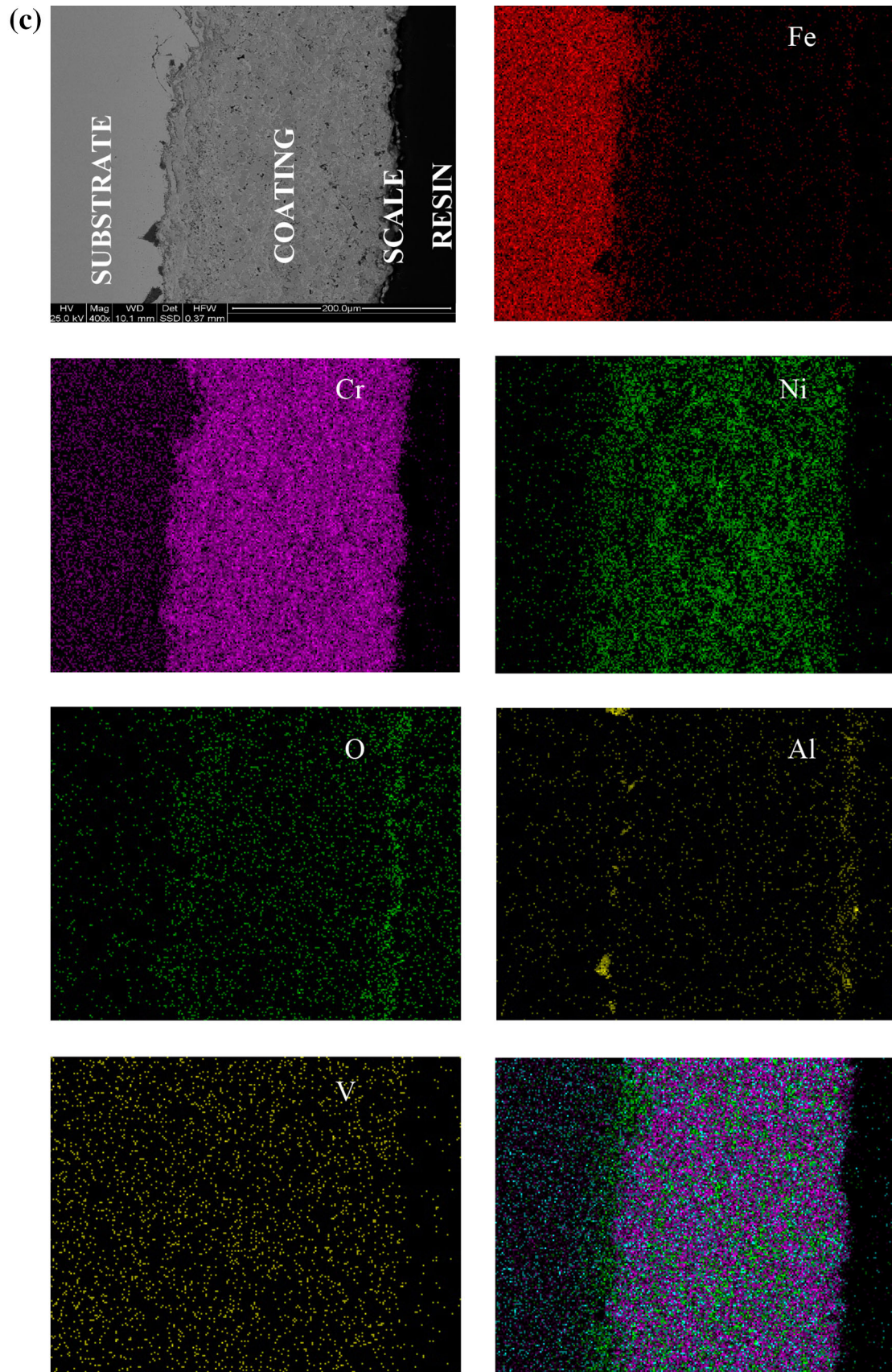


Fig. 5—continued.



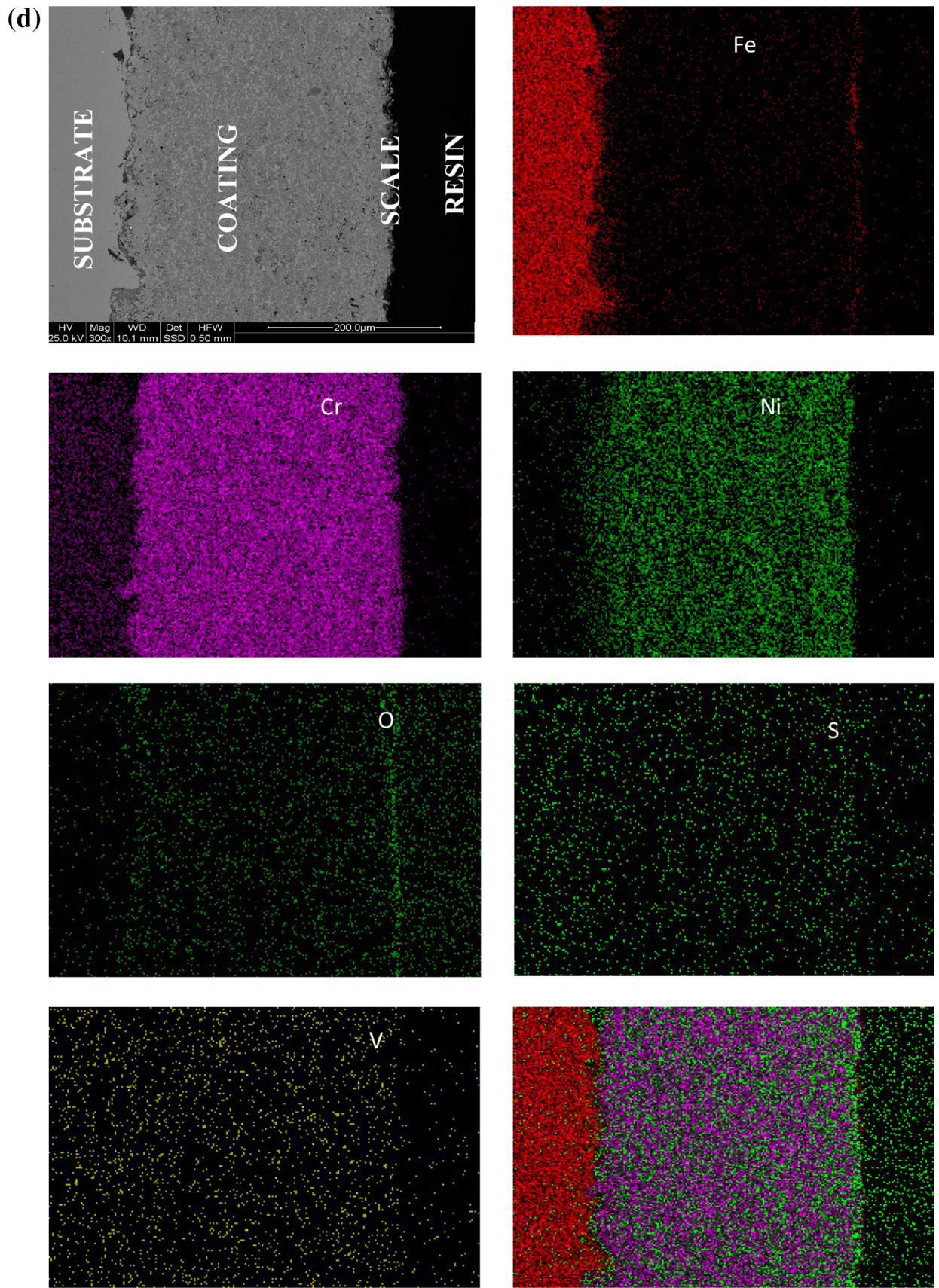


Fig. 5—continued.



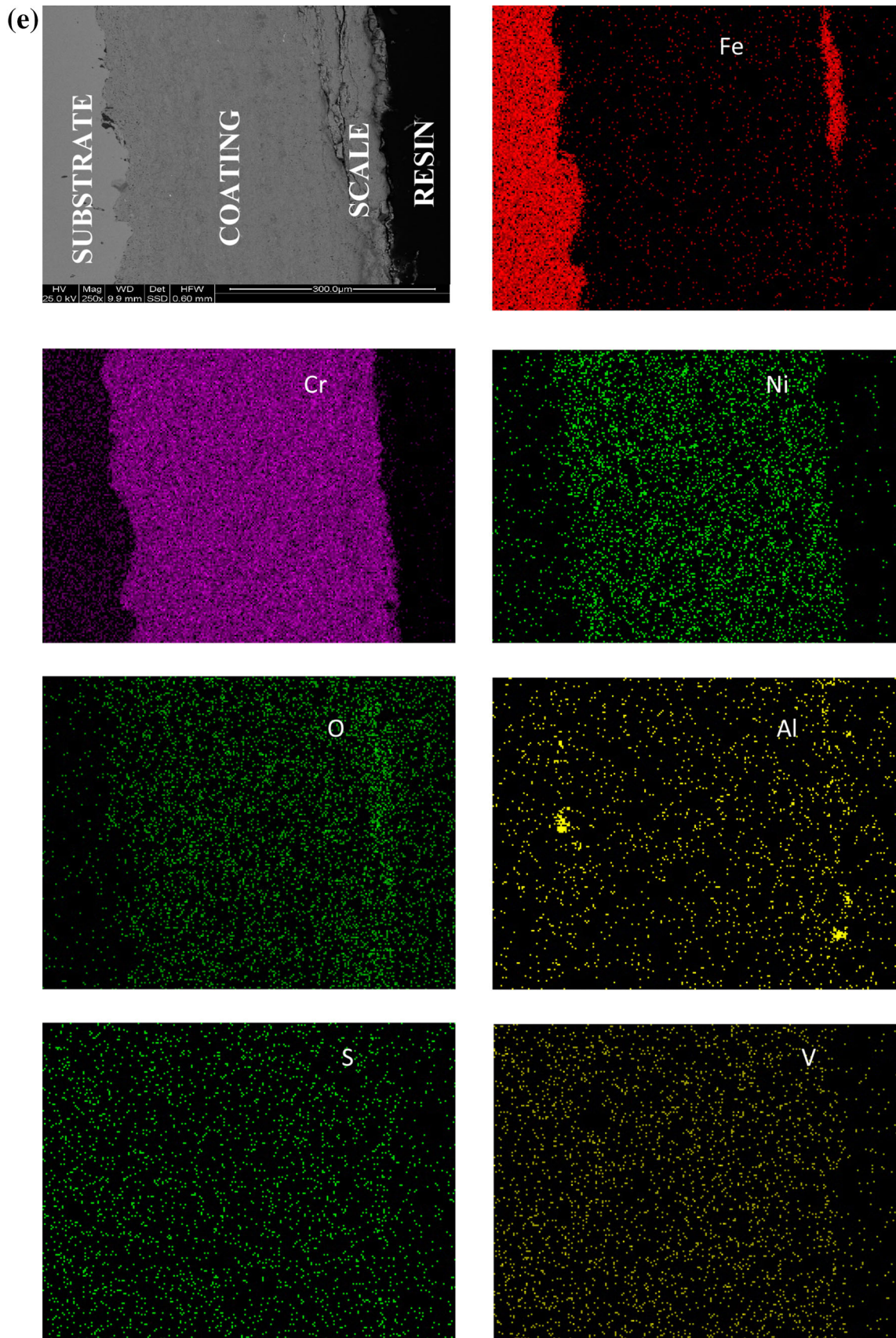


Fig. 5—continued.

Figure 5(b) further supports the results of XRD and EDAX analysis.

The embedded ash particles of Al can be clearly seen in the X-ray mapping shown in Figure 5(b). The main phases identified with XRD analysis  $\text{Al}_2\text{O}_3$ ,  $\text{Cr}_2\text{O}_3$ , NiCr,  $\text{Fe}_2\text{O}_3$  after 1500 hours exposure to the coal fired boiler environment. Kaur *et al.* in their studies regarding erosion corrosion resistance in an actual boiler environment have reported similar phases.<sup>[27]</sup> The cross-sectional EDAX analysis (Figure 4(b)) showed that the substrate steel is unaffected by the oxidation as the oxygen concentration at points 1 and 2 is only marginal. Fe is observed to be confined mainly to the base steel, which is a positive sign.

CC2 coating has shown resistance to the erosion corrosion in the given environment. This trend of thickness change may be due to the erosion of micro-hills present on the surfaces of the specimen, as the coal used in Indian power stations has large amounts of ash (about 50 pct), which contain abrasive mineral species, such as hard quartz (up to 15 pct), which increase the erosion propensity of coal.<sup>[37]</sup> However, once the surfaces became smooth, no further erosion-corrosion was noticed. This indicates the useful nature of the coating to control erosion-corrosion during longer durations of exposure. The phases revealed by XRD diffractograms are  $\text{Cr}_2\text{O}_3$  and  $\text{Al}_2\text{O}_3$ , along with  $\text{V}_2\text{O}_5$ ,  $\text{Cr}_3\text{C}_2$  and  $\text{Ni}_3\text{Fe}$  phases. The corrosion resistance of the coating in the given environment could be attributed to the formation of a continuous thick layer of  $\text{Cr}_2\text{O}_3$  in the top scale as indicated by the cross-sectional EDS and X-ray mapping analysis shown in Figs. 4(c) and 5(c), respectively. The presence of  $\text{Al}_2\text{O}_3$  might be due to the deposition of ash as discussed earlier.

The BSE image of the CC3-coated sample (Figure 4(d)) obtained after 1500 hours of exposure shows the formation of uniform and continuous oxide scales without any indications of any adherence loss between the coating and the substrates. The surface morphology shown in Figure 3(d) indicates the presence of Cr along with ash contents in the form of Al and Si. The scale formed shows granular growth with pits inbetween the mounds. The XRD analysis shows the presence of  $\text{Cr}_2\text{O}_3$  and  $\text{Al}_2\text{O}_3$ , along with some peaks corresponding to  $\text{Cr}_3\text{C}_2$  and  $\text{Fe}_2\text{O}_3$  phases. The presence of phases of Al and Fe in the top scale is confirmed by the X-ray mapping shown in Figure 5(d), indicating the formation of  $\text{Fe}_2\text{O}_3$  and  $\text{Al}_2\text{O}_3$ , which is further validated by the EDAX analysis shown in Figure 4(d).

Cracks parallel to the substrate surface are visible in the top layer of the CC4-coated sample as shown in the BSE image in Figure 3(e). These cracks might be due to some stresses generated in the scale due to differences in the specific volume of the oxides and the coating. Stresses can also develop with time as a result of mechanical/physical properties changes in the coating due to reaction with the corrosive environment as suggested by Heath *et al.*<sup>[38]</sup> They further opined that, due to stresses, cracks are formed in the scale and through these cracks the corrosive species reach the base metal quickly and cut its way under the coating to result in adhesion loss.

Oxide scale of the CC4-coated sample mainly comprises of phases of  $\text{Cr}_2\text{O}_3$  and  $\text{Al}_2\text{O}_3$ , along with  $\text{Cr}_7\text{C}_3$ ,  $\text{Fe}_2\text{O}_3$  and  $\text{SiO}_2$  phases after exposure to an actual boiler environment for 1500 hours. The EDAX analysis from cross-section and X-ray mappings analysis further confirmed the formation of a  $\text{Cr}_2\text{O}_3$  layer in the oxide scale as shown in Figs. 4(e) and 5(e), respectively. The presence of  $\text{Al}_2\text{O}_3$  and  $\text{SiO}_2$  may be due to ash deposited on the samples as discussed earlier. The presence of  $\text{Cr}_7\text{C}_3$  in the coated steel after oxidation might be the result of the high affinity of chromium toward carbon, which is well documented by Saunders *et al.*<sup>[39]</sup>

## V. CONCLUSIONS

- HVOF-sprayed  $\text{Cr}_3\text{C}_2$ -NiCr coatings were found to be effective in imparting erosion-corrosion resistance in a coal-fired boiler environment.
- Corrosion is more prominent as compared to erosion in the actual boiler environment. So, the CC1 coating has provided better degradation resistance than the remaining coatings, which may be due to the presence of a higher percentage of NiCr suitable for corrosion resistance and the  $\text{Cr}_3\text{C}_2$  phase sufficient enough to combat erosive attack.
- The formation of a continuous and thick  $\text{Cr}_2\text{O}_3$ -rich band just above the scale-substrate interface has mainly contributed to the better performance of CC1-coated steel in the coal-fired boiler environment. This thick oxide layer of chromium acts as a diffusion barrier to the inward diffusion of corrosive species.
- The higher percentage of  $\text{Cr}_3\text{C}_2$  phase in the CC4 coating resulted in crack development in the coating. Cracks initiate from the non bonded lamellar area and propagate under impact due to -relatively weak bonding.
- Coatings with low amounts of hard constituents ( $\text{Cr}_3\text{C}_2$ ) are more resistant to erosion-corrosion attack among those investigated. In the present study, 35 pct of  $\text{Cr}_3\text{C}_2$  hard phase in the NiCr matrix provided maximum resistance to erosion-corrosion in an actual boiler environment.

## REFERENCES

1. R. Blum: Advanced (700 °C) *PF Power Plants*, EC Contact No SF/1001/97/DK, 1997.
2. N.D. Evans, P.J. Maziasz, R.W. Swindeman, and G.D. Smith: *Scripta Mater.*, 2004, vol. 51, pp. 503-07.
3. T.S. Sidhu, S. Prakash, and R.D. Agrawal: *Surf. Coat. Technol.*, 2006, vol. 201, pp. 1602-1612.
4. M. Kaur and H. Singh: *Anti Corros. Methods Mater.*, 2008, vol. 55, pp. 86-96.



5. M.K. Weulersee, G. Moulin, P. Billard, and G. Pierotti: *Mater.Sci. Forum*, 2004, vols. 461–464, pp. 973–80.
6. H.W. Nelson, H.H. Krause, E.W. Ungar, A.A. Putnam, C.J. Slunder, P.D. Miller, J.D. Hummel, and B.A. Landry: *Pub. Pergamon Press and ASME*, New York, 1959.
7. A.V. Levy: *Corros. Sci.*, 1993, vol. 35, pp. 1035–43.
8. P.S. Sidky and M.G. Hocking: *Br. Corros. J.*, 1999, vol. 34, pp. 171–83.
9. C.J. Li and W.Y. Li: *Surf. Coat. Technol.*, 2003, vol. 167, pp. 273–83.
10. C.H. Lee and K.O. Min: *Surf. Coat. Technol.*, 2000, vol. 132, pp. 49–57.
11. B.S. Mann and V. Arya: *Wear*, 2001, vol. 249, pp. 354–60.
12. L. Zhao and E. Lugscheider: *Surf. Coat. Technol.*, 2002, vol. 162, pp. 6–10.
13. Y. Liu, T.E. Fischer, and A. Dent: *Surf. Coat. Technol.*, 2003, vol. 167, pp. 68–76.
14. B.S. Sidhu and S. Prakash: *J. Mater. Process. Technol.*, 2006, vol. 172, pp. 52–63.
15. D.W. Parker and G.L. Kutner: *J. Adv. Mater. Process.*, 1991, vol. 139, pp. 68–72.
16. R.W. Smith and R. Knight: *J. Mater.*, 1995, vol. 47, pp. 32–39.
17. W. Tillmann, E. Vogli, I. Baumann, G. Kopp, and C. Weihs: *J. Therm. Spray Technol.*, 2010, vol. 19, pp. 392–408.
18. S. Matthews, B. James, and M. Hyland: *Mater. Charact.*, 2007, vol. 58, pp. 59–64.
19. R. Bhatia, S.S. Chatha, H.S. Sidhu, and B.S. Sidhu: *Mater. Charact.*, 2010, vol. 4, pp. 57–62.
20. K. Stein: *Wear*, 1999, vol. 224, pp. 153–59.
21. S.S. Chatha, H.S. Sidhu, and B.S. Sidhu: *Surf. Coat. Technol.*, 2012, vol. 206, pp. 3839–50.
22. R. Bhatia, H.S. Singh, and B.S. Sidhu: *Int. J. Surf. Eng. Mater. Technol.*, 2012, vol. 3, pp. 39–47.
23. S. Prakash, S. Singh, and B.S. Sidhu: *Proc. Natl. Semin. Adv. Mater. Process.*, 9–10th Nov., IIT, Roorkee, India, 2001, pp. 245–53.
24. S. Srikanth, B. Ravikumar, S.K. Das, K. Gopalakrishna, K. Nandakumar, and P. Vijayan: *Eng. Failure Anal.*, 2003, vol. 10, pp. 59–66.
25. B. Singh: Ph.D. Thesis, Indian Institute of Technology Roorkee, 2003.
26. N. Bala: Ph.D. Thesis, Punjab Technical University, Jalandhar, 2010.
27. G. Kaushal, H. Singh, and S. Prakash: *Metall. Mater. Trans. A*, 2011, vol. 42A, pp. 1836–46.
28. M. Kaur, H. Singh, and S. Prakash: *J. Therm. Spray Technol.*, 2009, vol. 18, pp. 619–32.
29. G. Kaushal, H. Singh, and S. Prakash: *Oxid. Met.*, 2011, pp. 1–23.
30. T.S. Sidhu, S. Prakash, and R.D. Agrawal: *Sadhana*, 2009, vol. 34, pp. 299–307.
31. B.Q. Wang, G.Q. Geng, and A.V. Levy: *Surf. Coat. Technol.*, 1992, vols. 54–55, pp. 529–35.
32. A.R. Nicoll and G. Wahl: *Thin Solid Films*, 1983, vol. 95, pp. 21–34.
33. M.F. Stroosnijder, R. Mevrel, and M.J. Bennet: *Mater. High Temp.*, 1994, vol. 12, pp. 53–66.
34. A. Ul-Hamid: *Mater. Chem. Phys.*, 2003, vol. 80, pp. 135–42.
35. D. Toma, W. Brandl, and U. Koester: *Surf. Coat. Technol.*, 1999, vols. 120–121, pp. 8–15.
36. T. Sundararajan, S. Kuroda, T. Itagaki, and F. Abe: *ISIJ Int.*, 2003, vol. 43, pp. 95–103.
37. P.R. Krishnamoorthy and S. Seetharamu: *Proc. LIPREX-89*, Hyderabad, 1989.
38. G.R. Heath, P. Hiemgartner, G. Irons, R. Miller, and S. Gustafsson: *Mater. Sci. Forum*, 1997, vols. 251–54, pp. 809–816.
39. S.R.J. Saunders and J.R. Nicholls: *Thin Solid Films*, 1984, vol. 119, pp. 247–69.